

MEDIUM RANGE REMNANT THICKNESS GAUGING USING HIGH ORDER SHEAR HORIZONTAL WAVES

Aurélien Thon¹

École de technologie supérieure
Montréal, CA

Pierre Bélanger

École de technologie supérieure
Montréal, CA

ABSTRACT

The detection and sizing of corrosion is a crucial element in many industries. For instance, the petrochemical industry needs reliable, easy and rapid nondestructive testing methods to evaluate the remaining wall thickness in pipelines. Moreover, at pipe supports, the pipe is typically only partially accessible. It has been demonstrated in the literature that the cutoff frequency-thickness product of high order ultrasonic guided wave modes can be used in pitch-catch medium to long-range remnant thickness gauging. The capabilities of this technique depend on the number of excited modes and therefore various parameters such as the frequency content of the input signal, the thickness of the waveguide and the configuration of the probe. Using simulations and experiments this paper demonstrates the possibility of residual thickness gauging in a 10 mm aluminum plate using electromagnetic acoustic transducers.

Keywords: Ultrasound, Ultrasonic Guided Waves, Shear Horizontal Waves, EMAT

NOMENCLATURE

f	Frequency
k	Wavenumber
V_s	Bulk shear wave velocity
V_p	Phase velocity
ρ	Density
E	Young's modulus
ν	Poisson's ratio

1. INTRODUCTION

Corrosion is a common problem across multiple industries. This phenomenon, if it is not monitored, can lead to failures that are generally accompanied by damage to the immediate environment. The standard technique for quantitative evaluation of the remnant wall thickness remains point-by-point ultrasonic testing [1]. This technique allows a reliable measurement but is tedious. Point-by-point ultrasonic thickness gauging becomes

even more difficult at pipe supports when the pipe needs to be lifted for inspection. Possible solutions to this problem such as ultrasonic guided wave tomography are difficult to implement in practice due to the constraints associated with the dimensions, positions, and quantity of probes.

1.1 Wave Propagation

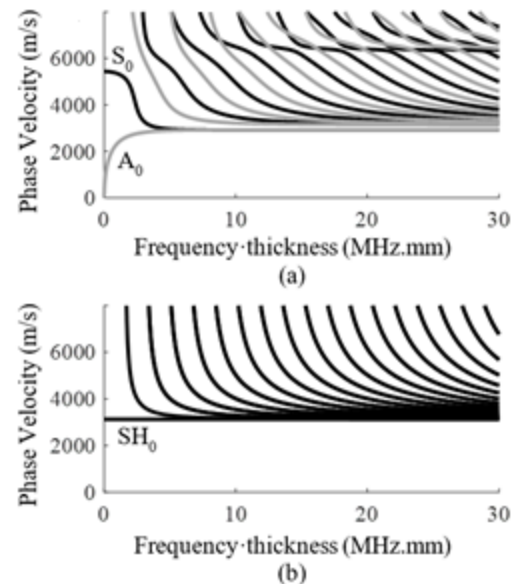


FIGURE 1: (a) Lamb wave phase velocity dispersion curves and (b) SH wave phase velocity dispersion curves in an aluminum plate ($\rho = 2700 \text{ kg/m}^3$, $E = 70 \text{ GPa}$, $\nu = 0.33$)

The solution investigated in this paper is the use of the cutoff frequency-thickness product of high order ultrasonic shear horizontal (SH) guided wave modes. The cutoff frequency-

¹ Contact author: aurelien.thon@pulets.ca

thickness product is a threshold below which a high order mode will not propagate. At this frequency-thickness product, the mode is either converted or reflected. The phase velocity of the high order mode tends to infinity and its group velocity towards zero. The dispersion curves of the different guided waves modes can easily be obtained using Disperse (Figure 1) [3]. Therefore, by exciting a large number of modes in a pitch-catch arrangement, it is possible to let the structure filter out the modes in accordance with the minimum thickness.

High order SH modes are evenly distributed in the frequency-thickness domain; this property allows an estimation of the minimum thickness on a regular grid. The cutoff frequency $f_{cutoff,n}$ of the n^{th} mode for a thickness h can easily be obtained with the following equation:

$$f_{cutoff,n} = \frac{nv_s}{2h}, n \in \mathbb{N} \quad (1)$$

It can be seen from this equation that increasing the frequency also increases the number of excited modes and hence the resolution of the technique. However, higher frequency results in higher attenuation and thus the inspection distance is reduced.

1.2 Transduction

EMAT (electromagnetic acoustic transducer) refers to a transducer technology using electromagnetic forces. The experiments showed in this paper were conducted on an aluminum plate to allow easier handling in the laboratory; Lorentz forces were therefore used. A transducer structure particularly suited to multimodal SH wave generation is the Periodic Permanent Magnet EMAT (PPM EMAT) (Figure 2).

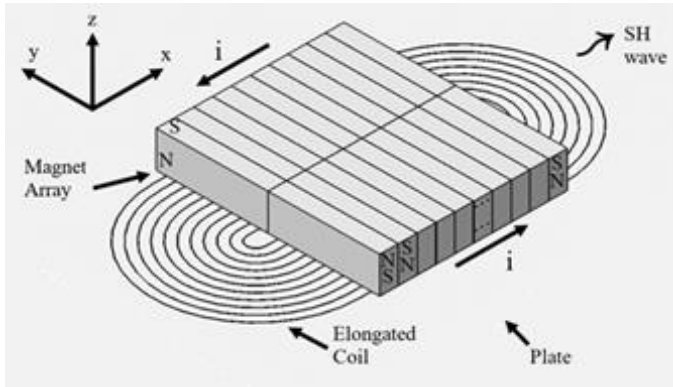


FIGURE 2: Schematic of a PPM EMAT

With a PPM EMAT, the size of the probe in the direction of propagation and therefore the number of magnets influences the wavelength selectivity of the transducer. The selectivity of the probe increases with the number of magnets.

All experiments and simulations presented in this paper were carried out with a 10 mm aluminum plate. The properties of aluminium were taken as: $\rho = 2700 \text{ kg/m}^3$, $E = 70 \text{ GPa}$ and $\nu = 0.33$. An arbitrary distance between the probes of 0.5 m was

chosen. An arbitrary minimum thickness in the inspection area was chosen as 5 mm. These values were used to calculate the cutoff frequencies of the first 4 SH modes:

TABLE 1: Cutoff frequencies of SH₁ to SH₄ in a 10 mm aluminum plate ($\rho = 2700 \text{ kg/m}^3$, $E = 70 \text{ GPa}$, $\nu = 0.33$) with a 5 mm thickness loss

Thickness	SH ₁	SH ₂	SH ₃	SH ₄
5 mm	313 kHz	626 kHz	939 kHz	1252 kHz
10 mm	156 kHz	313 kHz	469 kHz	626 kHz

In this paper the threshold below which a mode was considered as completely reflected or converted to a lower order mode was set to -20dB below the mode with the highest amplitude. When considering a 3 cycle Hann windowed toneburst centred at 500 kHz, the -20 dB bandwidth is from 225 to 775 kHz. Therefore, if the thickness reduces to 5 mm in a 10 mm waveguide, only SH₀ to SH₂ should be able to propagate.

2. MATERIALS AND METHODS

2.1 The waveguide and the defects

The waveguide used for the experiments was a 9.9 mm aluminum plate of dimensions 914 mm by 914 mm. Accelerated corrosion using a saline solution and electrodes was used to generate 5 mm deep defects.

2.2 The separation of modes

The signals generated by this method are complex due to their multimodal nature. A solution to separate the different modes is to make a series of regularly spaced measurements and perform a two-dimensional fast Fourier transform [4]. The wavenumber-frequency map can then be converted to a phase velocity-frequency map using:

$$V_p = \frac{2\pi f}{k} \quad (1)$$

2.3 Finite element simulations

The simulations carried out to design and predict the capabilities of the EMAT were made on a 10 mm thick aluminum plate. In order to model the defects, the surface of the experimental plate was scanned with a Metrascan 3D Optical Scanner.

The simulation of this multiphysics problem was carried out in two stages. First, the Lorentz forces were calculated on Comsol Multiphysics 5.3. Then the forces were imported into Pogo [5]; a GPU accelerated finite element simulation code solving the elasto-dynamic equation of wave propagation. To minimize the error, 15 elements per wavelength were used.

2.4 The experimental setup

The EMAT manufactured was designed to have a centre frequency of 500 kHz and a pitch of 3.2 mm and comprised 20x2 neodymium magnets of grade N42 (25.4 mm by 6.4 mm by 3.2

mm). The coil was printed on a PCB to guarantee the orientation of the magnets and the coil.

The signal provided to the EMAT was generated by an Agilent 33500B signal generator and amplified by a Ritec RPR-4000 High Power Pulser Receiver. The reception was handled by a dual-laser Doppler vibrometer system and a high-definition 4-channel oscilloscope DSO9024H. The measurement was automated using an XY table.

3. RESULTS AND DISCUSSION

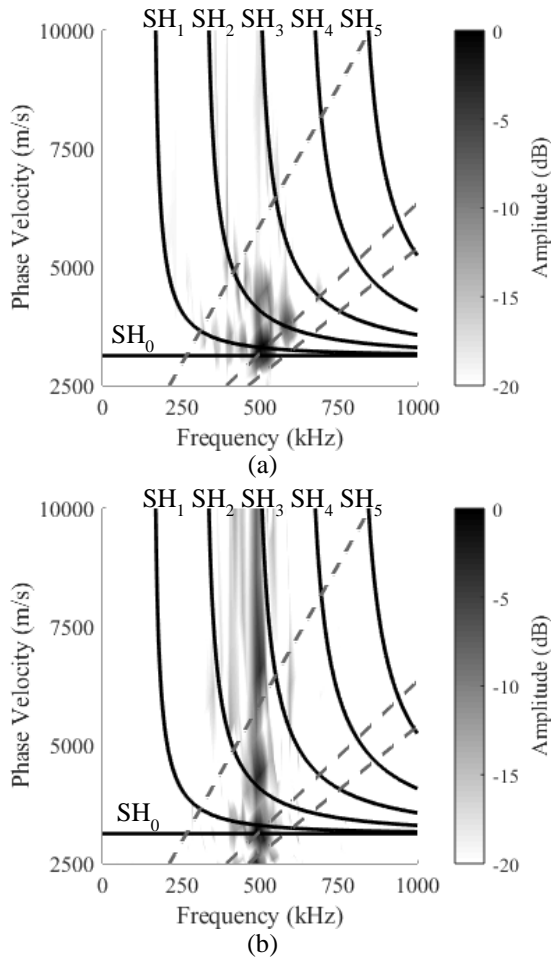


FIGURE 3: 2D Fourier transform of signals extracted from experimental measurements shown in a phase velocity and frequency map. (a) No defect (b) 130 mm by 80 mm defect. The top and bottom diagonal grey dashed lines correspond to the wavenumber bandwidth of the EMAT. The centerline corresponds to the wavenumber associated with the pitch of the magnet

Figure 3 (a) shows the energy distribution when there were no defects along the propagation path and Figure 3 (b) presents the energy distribution when the propagation is through a 130 mm by 80 mm and 5 mm deep accelerated corrosion patch.

According to the prediction made with Table 1 in a defect-free plate, all modes from SH₀ to SH₄ should propagate. However, the amplitude of SH₄ was too low to be detected. It can be explained by the fact that this mode is close to the maximum excited frequency when using a threshold of -20 dB.

When comparing figure 3 (a) and (b), it is possible to see that the highest order propagating mode was SH₁. As SH₂ was filtered out by the defect and using Eq. 1 it is possible to evaluate the minimum remnant thickness along the propagation path to be under 5.1 mm. SH₁ was still propagating which implied that the minimum remnant thickness was above 3 mm. This result is in accordance with the true minimum remnant thickness of 5 mm.

4. CONCLUSION

The use of an EMAT in the generation of a multimodal SH wave packet was carried out. Then using the cutoff frequencies of the high order SH modes the minimum remnant thickness along the propagation path was estimated to be between 3 mm and 5.1 mm. The actual thickness in the middle of the accelerated corrosion patch was 5 mm.

ACKNOWLEDGEMENTS

We would like to thank Nvidia for providing us with a Nvidia Quadro P6000 graphics card for our GPU simulations. The authors would also like to thank the Natural Sciences and Engineering Research Council of Canada and Olympus NDT Canada for funding this project.

REFERENCES

- [1] Krautkrämer, J., and Krautkrämer, H., 1990, *Ultrasonic Testing of Materials*, Springer Berlin Heidelberg, Berlin, Heidelberg.
- [2] Belanger, P., 2014, "High Order Shear Horizontal Modes for Minimum Remnant Thickness," *Ultrasonics*, **54**(4), pp. 1078–1087.
- [3] Pavlakovic, B., Lowe, M., Alleyne, D., and Cawley, P., 1997, "Disperse: A General Purpose Program for Creating Dispersion Curves," *Review of Progress in Quantitative Nondestructive Evaluation*, Springer, Boston, MA, pp. 185–192.
- [4] Alleyne, D., and Cawley, P., 1991, "A Two-Dimensional Fourier Transform Method for the Measurement of Propagating Multimode Signals," *The Journal of the Acoustical Society of America*, **89**(3), pp. 1159–1168.
- [5] Huthwaite, P., 2014, "Accelerated Finite Element Elastodynamic Simulations Using the GPU," *Journal of Computational Physics*, **257**, pp. 687–707.